Universal Modeling of the Bulk Acoustic Wave Devices

Boris Sveshnikov
State University
Nizhny Novgorod, Russia
bvs@ieee.org

***Abstract*—Highly efficient self-consistent 1D-model is proposed allowing us to describe arbitrary BAW devices, including the tunable ones. Applying that approach one can analyze, in the frame of the same software, a system with arbitrary number and sequence of dielectric and metal layers under arbitrary inter-electrode connections. It is shown that one can fluently control the resonant frequency of solidly mounted BAW resonator over a fractional frequency range > 1% (being much wider than the system temperature drift).**

I. Introduction

Thin film (FBAR) and solidly mounted (SMR) bulk wave resonators are widely used in the modern wireless communication networks [1,2]. FEM-BEM analysis, being able to describe them precisely, is the rather cumbersome and time-consuming procedure.

Flexible and fast simulation of BAW devices in one-dimensional (1D) form is a correct and rigorous approach, if the propagation of the wave of interest is along an axis of symmetry of a crystal [3]. This is so at least in case of the widely used orientations of ZnO, AlN, W, Mo, W, Ti, Al.

The main disadvantage of 1D-theory is inability to take into account the spurious lateral modes (SLM) in FBAR/SMR devices. However, usage of irregular polygon electrode, in which no two sides are parallel to one, allows the considerable suppression of SLM in similar systems [4]. Thus, when utilizing the 1D-modeling, one should only introduce properly (on the phenomenological level) the relevant attenuation coefficients to take into account losses caused by non-synchronous excitation of the spurious modes.

Nevertheless, to the best of the author's knowledge, till now neither known 1D approach is able to simulate arbitrary FBAR/SBAR systems.

The self-consistent 1D - theory is developed presently to describe any BAW device. Applying this approach one can analyze, in the frame of the same software, systems with arbitrary number and sequence of dielectric and metal layers under arbitrary inter-electrode connections. The electrodes may compose an arbitrary spatial distribution of various electrical circuits, including tunable re-radiator loaded by variable admittance Yo [5].

II. Simulation Principles

In order to carry out quantitative calculations in multi-layered dissipative BAW system, we must state the relevant equation of motion and constitutive relations, reducing them afterwards to one-dimensional terms for the considered bulk mode (longitudinal or shear), in every j-th layer (j=1…N):

$$\frac{\partial T_j}{\partial x} = \rho_j \cdot \frac{\partial^2 u_j}{\partial t^2} \tag{1}$$

$$\begin{cases} T_j = c_j \cdot S_j + \eta_j \cdot \dfrac{\partial S_j}{\partial t} - \beta_j \cdot E_j & (2) \\ D_j = \varepsilon_j \cdot E_j + \beta_j \cdot S_j & (3) \end{cases}$$

Here T_j = stress, $S_j = \partial u_j/\partial x$ = strain, u_j = elastic displacement, D_j = electric displacement in the presence of electric field E_j ($\frac{\partial D_j}{\partial x} = 0$ [1]), c_j = the elastic constant, β_j = piezoelectric stress constan, η_j = coefficient of viscosity, ε_j = permittivity, and ρ_j = mass density of j-th layer [3]. Assuming the harmonic solution and omitting the factor $e^{i\omega t}$, one can simply transform system (1-3) to the following wave equation:

$$\frac{\partial^2 T_j}{\partial x^2} + q_j^2 \cdot T_j = -q^2 \frac{\beta_j}{\varepsilon_j} D_j \quad , \tag{4}$$

where $q^2 = \dfrac{\omega^2 \cdot \rho_j}{\tilde{c}_j}$, $\tilde{c}_j = c_j(1 + k_j^2) + i\omega\eta = c_j\left(1 + k_j^2 + i \cdot \dfrac{\varsigma_j}{\pi}\right)$,

while $k_j^2 = \dfrac{\beta_j^2}{\varepsilon_j \cdot c_j}$ and $\varsigma_j = \pi \dfrac{\omega \eta_j}{c_j}$ denote, respectively, the layer piezoelectric coupling constants and the attenuation coefficients characterizing acoustic losses per wavelength.

By analogy with the "SEA" approach, applied earlier to simulate SAW devices [6], let operate with the sequential "end-to-end" subscripting of wave amplitudes instead of the block-structured one used previously [7,8]: index of the "backward" wave comes to hand from an index of the "forward" wave in the

[1] Excepting neighbor edges of electrodes with different polarity.

978-1-4244-3510-4/09/$25.00 ©2009 IEEE

same layer simply by adding N-figure, where N is a number of the system layers, including electrodes and substrate.

The searched fields may be represented as follows:

$$u_j(x) = U_j e^{-i\cdot q\cdot(x-x_{j-1})} + U_{j+N} e^{i\cdot q\cdot(x-x_{j-1})}, \text{ if } x_{j-1} \le x \le x_j \qquad (5)$$

At this point we can write: $T_j = \tilde{c}_j \cdot \frac{du_j}{dx} - \frac{\beta_j}{\varepsilon_j} \cdot D_j$.

All the acoustic amplitudes U_m are found satisfying all the elastic and electric boundary conditions at interfaces $x_1 \ldots x_{N-1}$, giving us '2N-2' equations, plus two boundary conditions at the edges $x = 0$ and $x = x_N$, which may be either rigidly clamped ($BC_{1,2} = -1 \Leftrightarrow u(x_{0,N}) = 0$), or free ($BC_{1,2} = 1 \Leftrightarrow T(x_{0,N}) = 0$):

$$\begin{cases} U_{j+1} + U_{j+N} \cdot e^{i\cdot q_j\cdot d_j} = U_j \cdot e^{-i\cdot q_j\cdot d_j} + U_{j+N+1} \\ U_{j+1} + \frac{Z_j}{Z_{j+1}} U_{j+N} e^{i\cdot q_j\cdot d_j} = \frac{Z_j}{Z_{j+1}} U_j e^{-i\cdot q_j\cdot d_j} + U_{j+N+1} + \frac{i\cdot D_j}{\omega Z_{j+1}}\left(\frac{\beta_{j+1}}{\varepsilon_{j+1}} - \frac{\beta_j}{\varepsilon_j}\right) \end{cases} \qquad (6)$$

if $1 < j < N$, and

$$\begin{cases} U_1 = BC_1 \cdot U_{N+1} + \frac{i\cdot\beta_1 D_1}{2\varepsilon_1\omega Z_1}(1 + BC_1) \\ U_{2N} = BC_2 \cdot e^{-i\cdot 2q_N\cdot d_N} \cdot U_N - \frac{i\cdot\beta_N D_N}{2\varepsilon_N\omega Z_N}(1 + BC_2)\cdot e^{-i\cdot q_N\cdot d_N} \end{cases} \qquad (7)$$

The denotations $Z_j = \sqrt{\rho_j \tilde{c}_j}$ and $d_j = x_j - x_{j-1}$ (x_0=0) are used above. The scattering coefficients, characterizing the backward ($r_j^{(+)}$) and forward ($r_j^{(-)}$) wave reflections, as well as the backward ($t_j^{(-)}$) and forward ($t_j^{(+)}$) wave transmission, at j-th cross-section may be expressed as follows:

$$r_j^{(\pm)} = \pm\frac{Z_{j+1} - Z_j}{Z_{j+1} + Z_j}; \quad t_j^{(\pm)} = \frac{2Z_{j,j+1}}{Z_{j+1} + Z_j} \qquad (8)$$

So, the system of equalities (6) may be rewritten in the physically clear form, similarly to the "SEA" manner:

$$\begin{cases} U_{j+1} = r_j^{(+)} U_{j+N+1} + t_j^{(+)} \cdot e^{-i\cdot q_j\cdot d_j} U_j + \frac{i\cdot D_j}{\omega(Z_{j+1}+Z_j)}\left(\frac{\beta_{j+1}}{\varepsilon_{j+1}} - \frac{\beta_j}{\varepsilon_j}\right) \\ U_{j+N} = r_j^{(-)} e^{-2i\cdot q_j\cdot d_j} \cdot U_j + t_j^{(-)} \cdot e^{-i\cdot q_j\cdot d_j} U_{j+N+1} + \frac{i\cdot D_j \cdot e^{-i\cdot q_j\cdot d_j}}{\omega(Z_{j+1}+Z_j)}\left(\frac{\beta_{j+1}}{\varepsilon_{j+1}} - \frac{\beta_j}{\varepsilon_j}\right) \end{cases} \qquad (9)$$

Thus, bearing in mind (7), one can rewrite the boundary conditions in the matrix form $\vec{U} = \hat{M} \cdot \vec{U} + \vec{H}$, solving it at a blow:

$$\vec{U} = (\hat{I} - \hat{M})^{-1} \cdot \vec{H} \qquad (10)$$

The found amplitude distribution of acoustic fields allows determination of the charges and, therefore, currents induced on electrodes under given voltage. In particular, an admittance of transducer, formed by any two electrodes, whose nearest to each other sides are placed at the co-ordinates x_{n1} and x_{n2} ($x_{n2} > x_{n1}$), is defined by the following expression:

$$Y = \frac{i\cdot\omega\cdot\Xi}{\sum_{j=n1}^{n2} \frac{1}{\varepsilon_j}\left\{d_j - \beta_j \cdot \left[u_j(x_j) - u_j(x_{j-1})\right]\right\}} \qquad (11)$$

A character 'Ξ' above denotes the electrode area.

III. Tunable SMRs and Those Based Filters

Let us consider a simple (not optimized) example of the solidly mounted resonator (SMR) containing two transducers (BWTs) formed by three Al electrodes and two piezoelectric ALN layers between them. One of transducers (with free top surface: $BC_1 = 1$) is connected to external circuitry as one-port network, though another BWT serves as a tunable reflector (Figure 1).

The second transducer, loaded by variable reactance, is mounted on the melted Quartz substrate (with rigidly clamped bottom: $BC_2 = -1$). An intermediate acoustical Bragg reflector of alternating high and low acoustic impedance layers W and SiO_2, assumed to be manufactured there in order to select only one acoustic resonance in this potentially multi-resonant system.

NB: Voltage drop on the re-radiator load Yo, drawn in Fig.1, is expressed through both Yo-value and the U-distribution within the re-radiator domain, contributing to the relevant terms of matrix **M**.

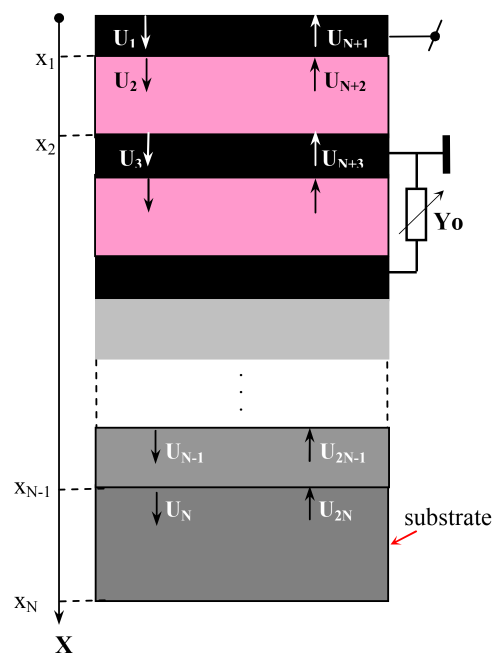

Figure 1. Conventional image of SMR with 3 electrodes (layers ## 1,3, 5).

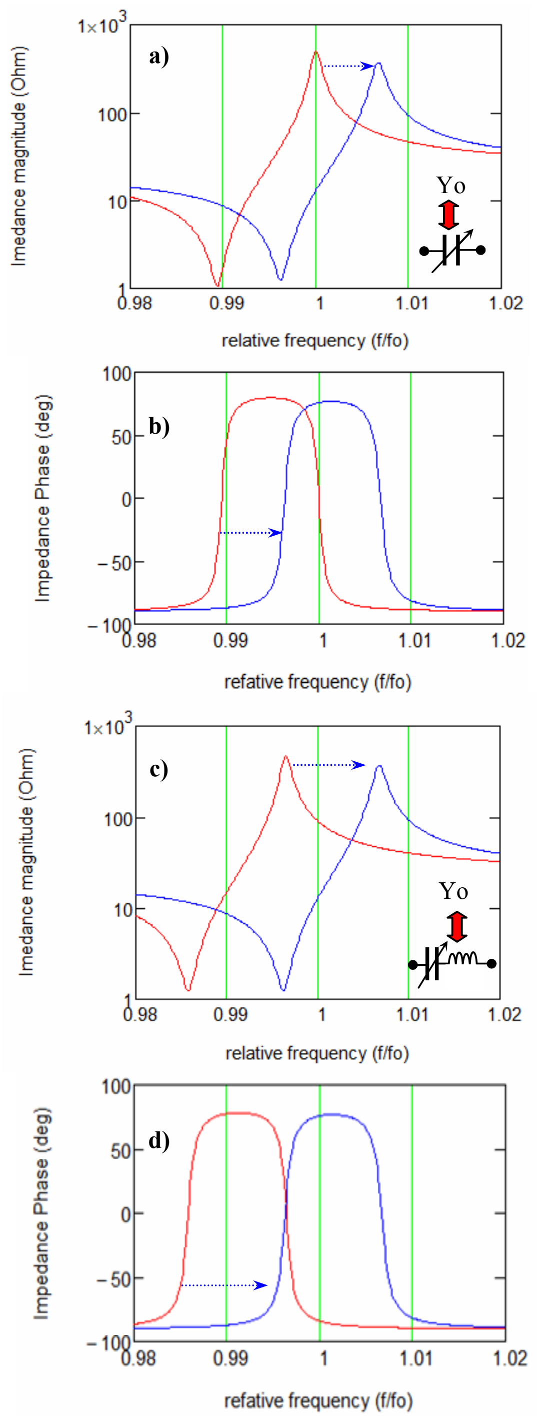

Figure 2. Impedance of tunable SMR with pure capacitive (a,b) and combined (c,d) electric load of the phase-shifting reflector.

One can control admittance Yo (containing, e.g., the variable capacitor) and change the reflection coefficient phase - at the interface x = x_2 on Fig.1 - over an interval $0 \le \Delta\varphi \le 2\pi$ [5]. That is, the maximal possible tuning range of the considered SMR is equal to the frequency "gap" between its longitudinal eigenmodes. Only the ohm losses in a load with finite Q-factor are able to restrict the tuning efficiency.

Figures 2a,b illustrate tunability of similar SMR (under N=21), achieved by using only variable capacitor (with quality factor Qc=300). At the same time, Figures 2c,d demonstrate how the tuning range may be increased at the expense of additional inductor with Q-factor equaled to QL=50. We assume here that attenuation coefficients per wavelength in all layers have the same value equaled to $\varsigma_0 = 3\cdot10^{-3}$ neper[2].

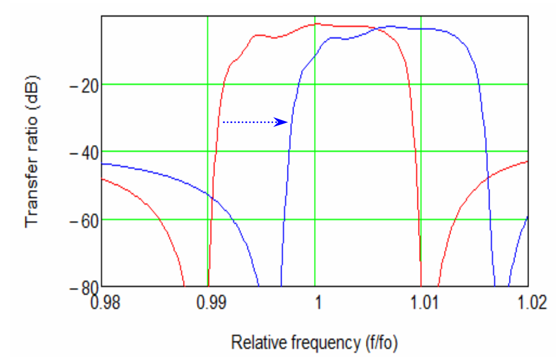

Figure 3. Frequency response of the tunable SMR based filter with variable capacitor as electrical load (corresponding to Figures 2a,b).

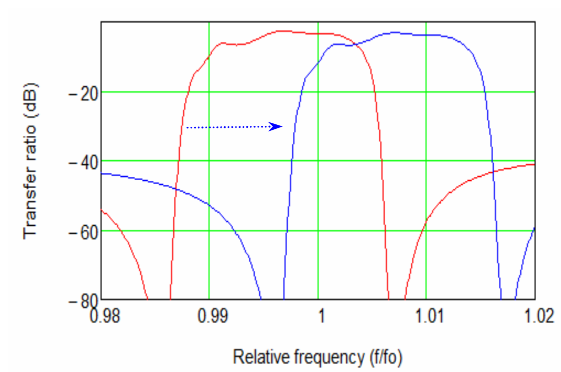

Figure 4. Tuning of the SMR based filter with help of additional inductor (corresponding to Figures 2c,d).

By using those resonators as impedance elements (with properly shifted resonances) it is possible to form a "stage" of ordinary ladder type filter. Frequency response of similar filter

[2] Naturally, in reality one has to estimate these figures with more accuracy.

(**not optimized**), containing a number (n=5) of identical tunable stages, is drawn on Figures 3 and 4.

IV. Conclusion

The very flexible 1D model is developed to facilitate and accelerate simulation and optimization of various BAW devices, taking into account unavoidable dissipation of acoustic energy.

A method is proposed and investigated numerically allowing design of the tunable SMRs, as well those based Low-Loss filters. It is shown that one can control the central frequency of similar systems in a rather wide relative interval (~ 1%) without notable deterioration of the device performances.

References

[1] K.M. Lakin, "Thin film resonators and filters", IEEE Ultrasonics Symposium Proceedings, 1999, pp. 895-906.

[2] R.Ruby, P.Bradley, Y.Oshmyansky, A.Chien, "Thin Film Bulk Wave Acoustic Resonators (FBAR) for Wireless Applications", IEEE Ultrasonics Symposium Proceedings, 2001, pp.813-821.

[3] G.S. Kino, Acoustic waves: Devices, Imaging and Analog Signal Processing, Prentice-Hall, Inc. Englewood Cliffs, New Jersey, 2000.

[4] US Patent # 6.215.375.

[5] B.V. Sveshnikov, "Tunable Phase-Shifting Reflectors of Surface and Bulk Acoustic Waves", Ultrasonics World Congress Proceedings, Berlin, 1995, pp. 387-390.

[6] B.V.Sveshnikov and A.P.Shitvov, "On universal two-dimensional modeling of SAW devices with complex architectures", IEEE Ultrasonics Symposium Proceedings, 1999 , pp. 113-118

[7] H. Nowotny, E. Benes, "General one-dimensional treatment of the layered piezoelectric resonator with two electrodes", J. Acoust. Soc. No 2, August 1987, pp. 513-521.

[8] V.Y. Zhang, B. Dubus, J.E. Lefebvre, and T. Gryba, "Modeling of bulk acoustic wave devices built on piezoelectric stack structures: impedance matrix analysis and network representation", IEEE Trans. on UFFC, v. 55, no. 3, 2008, pp. 704-716.